Published in final edited form as:
Ann Neurol. 2012 November ; 72(5): 750–765. doi:10.1002/ana.23670.

STAT3-mediated astrogliosis protects myelin development in neonatal brain injury

Hiroko Nobuta, Ph.D.[1,2], **Cristina A. Ghiani, Ph.D.**[1,3], **Pablo M. Paez, Ph.D.**[1,3], **Vilma Spreuer, B.S.**[1,3], **Hongmei Dong, B.S.**[1,3], **Rose A. Korsak, B.A.**[4], **Armine Manukyan, B.S.**[1,3], **Jiaxi Li**[1,3], **Harry V. Vinters, M.D.**[5], **Eric J. Huang, M.D., Ph.D.**[6,7], **David H. Rowitch, M.D., Ph.D.**[8,9], **Michael V. Sofroniew, M.D., Ph.D.**[4], **Anthony T. Campagnoni, Ph.D.**[1,3], **Jean de Vellis, Ph.D.**[1,3,4], and **James A. Waschek, Ph.D.**[1,2,3]

[1]Semel Institute for Neuroscience and Human Behavior, Department of Psychiatry and Biobehavioral Sciences, David Geffen School of Medicine, University of California, Los Angeles, Los Angeles, CA 90095, USA

[2]Interdepartmental Graduate Program in Neuroscience, University of California, Los Angeles, Los Angeles, CA 90095, USA

[3]Intellectual and Developmental Disabilities Research Center, David Geffen School of Medicine, University of California, Los Angeles, Los Angeles, CA 90095, USA

[4]Department of Neurobiology, David Geffen School of Medicine, University of California, Los Angeles, Los Angeles, CA 90095, USA

[5]Departments of Pathology and Laboratory Medicine and Neurology, University of California, Los Angeles, Los Angeles, CA 90095, USA

[6]Pathology Service, Veterans Affairs Medical Center, San Francisco, CA 94121, USA

[7]Department of Pathology, University of California San Francisco, 513 Parnassus Avenue, San Francisco, CA 94143, USA

[8]Departments of Pediatrics and Neurosurgery, Eli and Edythe Broad Institute for Stem Cell Research and Regeneration Medicine and Howard Hughes Medical Institute, San Francisco, CA 94143, USA

[9]Division of Neonatology, University of California San Francisco, 513 Parnassus Avenue, San Francisco, CA 94143, USA

Abstract

Objective—Pathological findings in neonatal brain injury associated with preterm birth include focal and/or diffuse white matter injury (WMI). Despite the heterogeneous nature of this condition, reactive astrogliosis and microgliosis are frequently observed. Thus, molecular mechanisms by which glia activation contribute to WMI were investigated.

Methods—Postmortem brains of neonatal brain injury were investigated in order to identify molecular features of reactive astrocytes. The contribution of astrogliosis to WMI was further tested in a mouse model in genetically-engineered mice.

Results—Activated STAT3 signaling in reactive astrocytes was found to be a common feature in postmortem brains of neonatal brain injury. In a mouse model of neonatal WMI, conditional

Correspondence: James A. Waschek, Ph.D., University of California, Los Angeles, 635 Charles E. Young Dr. South, Neuroscience Research Bldg Room 345, Los Angeles, CA 90095-7332, tel (310) 825-0179, fax (310) 206-5061, jwaschek@mednet.ucla.edu.

deletion of STAT3 in astrocytes resulted in exacerbated WMI, which was associated with delayed maturation of oligodendrocytes. Mechanistically, the delay occurred in association with over-expression of TGFβ-1 in microglia, which in healthy controls, decreased with myelin maturation in age-dependent manner. TGFβ-1 directly and dose-dependently inhibited the maturation of purified oligodendrocyte progenitors, and pharmacological inhibition of TGFβ-1 signaling in vivo reversed the delay in myelin development. Factors secreted from STAT3-deficient astrocytes promoted elevated TGFβ-1 production in cultured microglia compared to wild type astrocytes.

Interpretation—These results suggest that myelin development is regulated by a mechanism involving cross-talk between microglia and oligodendrocyte progenitors. Reactive astrocytes may modify this signaling in STAT3-dependent manner, preventing the pathological expression of TGFβ-1 in microglia and the impairment of oligodendrocyte maturation.

Introduction

Oligodendrocytes (OL) are the myelinating cells of the central nervous system, facilitating fast conduction of action potentials along the axon. In humans, myelin development begins prenatally and continues into young adulthood to achieve complex neurological functions. Failure of proper myelin development is a common pathology in neonatal brain injury associated with preterm and term births associated with hypoxic-ischemia or other insults[1–7]. The pathology, collectively called neonatal white matter injury (WMI), ranges from diffuse non-necrotic changes affecting mainly subcortical white mater (hypoxic-ischemic encephalitis, HIE) to focal lesions affecting periventricular white matter (periventricular leukomalacia, PVL), and is characterized by underdeveloped myelin and wide-spread reactive gliosis, along with limited neuronal loss in some cases. Afflicted children frequently present with diminished cognitive, motor, and psychiatric functions that persist beyond infancy[8–10]. Although etiology of WMI is likely to be multifactorial, neuroinflammation appears to be a major contributing factor, as suggested by consistent positive correlation with infections during pregnancy[11, 12] and postnatal period[13], elevation of immune activity in the fetal blood[14], amniotic fluid[15], and umbilical cord[16]. Despite these findings, limited knowledge with respect to the causal link and molecular mechanisms by which such insults lead to actual damages to oligodendrocytes has hindered the development of effective therapies.

Similar to many adult disorders of the central nervous system (CNS), reactive gliosis (astrocyte and microglia activation) is a hallmark of neonatal WMI[17–20]. In adult CNS, astrocytes are known to play homeostatic roles in active maintenance and surveillance of CNS environment, and in activated state, play putative roles in both destruction and promotion of repair (reviewed in [21]). However, it is unclear if developing glial cells possess similar phenotypes and functions in the unique environment of the neonatal brain, and in particular, whether they have direct contribution to the pathology observed in WMI. In fact, recent evidence suggests that an arrest in OL maturation, rather than cellular loss, underlies some cases of WMI[22, 23], raising the possibility that the pathological brain environment may be inhibitory for OL differentiation, leading to growth failure and improper damage repair. The purpose of this study was to identify cellular/molecular mechanisms of reactive gliosis underlying WMI in the neonatal brain, and to determine the consequences to myelin development. We report suporting evidence that STAT3-mediated astrogliosis plays a protective role in WMI, by restricting the aberrant expression of microglial TGFβ-1, a factor we found to inhibit OL maturation. These studies highlight not only a possible involvement of microglial signals in normal development of myelin, but also a protective role of astrogliosis in WMI involving microglial TGFβ-1.

Methods

Human postmortem brain tissues

All human tissues were collected as part of University of California Multicampus Research Programs and Initiatives. They were collected in accordance with guidelines established by the University of California San Francisco and University of California Los Angeles Committees on Human Research. Four cases of WMI (case 1–4) and three cases of controls (case 5–7) were analyzed (see Table 1). Cases 1 and 2 were 35 and 37 and 4/7 weeks of gestation respectively, with diagnoses of hypoxic-ischemic encephalopathy (HIE). Cases 3 and 4 were 31 weeks and 38 weeks of gestation, respectively, with diagnoses of periventricular leukomalacia (PVL). Control case 5 was 36 and 4/7 weeks, and case 6 was 37 and 3/7 weeks of gestations, and the causes of death were diaphragmatic hernia. Control case 7 was 38 weeks of gestation, suggestive but not diagnosis of acute anoxia. Brain tissues were harvested within 48 hrs of patient death, and were fixed in 4% paraformaldehyde, cryoprotected in sucrose solution (cases 1,2,5,6), embedded in OCT, sectioned, and stored at −72°C or fixed in neutral buffered formalin (cases 3,4,7), paraffin embedded, and sectioned, and stored at 4°C. Subcortical white matter below cingulate gyrus or periventricular white matter outside necrotic lesion was used for immunohistochemistry. Please see supplementary materials for additional information on diagnoses.

In vivo LPS treatment in mice

Experiments were performed according to protocols approved by the Chancellor's Animal Research Committee of the Office for Protection of Research Subjects at the University of California, Los Angeles. LPS (Escherichia coli strain O55:B5, lot number 20316A1) was purchased from List Laboratories. We determined that the concentration of 10 mg/kg in this lot was adequate to induce the white matter injury in C57BL/6 mice as described in the results. LPS was diluted in sterile saline to a concentration of 0.5 mg/ml and injected subcutaneously between the shoulders. Please see supplementary materials for detailed information on injection.

Conditional STAT3-deficient mice

The generation of mice deficient in STAT3 selectively in astrocytes was described previously[24–26]. The breeding strategy used in the experiments was $GFAPCre^{+}/STAT3^{loxploxp} \times GFAPCre^{-}/STAT3^{loxploxp}$. The offspring were approximately 50% $Cre^{+}/STAT3^{loxploxp}$ and 50% $Cre^{-}/STAT3^{loxploxp}$. All lines were backcrossed to C57BL/6 for at least eight generations, and littermates served as genotype controls. $GFAPCre^{+}$ mice were also bred with a reporter line expressing β-galactosidase [27]. C57Bl/6 WT mice were obtained from our ongoing breeding colony.

In vivo TGFβ receptor kinase inhibitor treatment in mice

A selective TGFβ receptor kinase inhibitor SB431542 (Cayman chemical) was dissolved in Dimethyl Sulfoxide and sterile saline (1:1 vol/vol) to a concentration of 0.5 mg/ml. An intraperitoneal injection at 5 mg/kg was administered at P2.

Western blot

Mouse forebrain at specified ages was homogenized in RIPA buffer containing protease inhibitor cocktail (mini complete, Roche). 25–35 ug of protein was resolved on a 4–20% gradient polyacrylamide gel (invitrogen) and transferred to PVDF membranes (Biorad). Membranes were then incubated with primary antibodies, appropriate secondary antibody conjugated to horseradish peroxidase, and visualized using ECL or ECL plus (GE healthcare). Quantification of relative amounts of proteins was made in ImageJ from

developed films. Primary antibodies used are: mouse MBP (1:1000, Covance), rabbit phosphorylated SMAD2 (1:500; Cell Signaling), mouse phosphorylated STAT3 (1:500, BD Biosciences), rat GFAP (1:2500, Invitrogen), and mouse β-actin (1:3000; Sigma).

Immunohistochemistry in human samples

All human postmortem WMI samples were subjected first to antigen retrieval protocol which consisted of a 10-min incubation in 10 mM sodium citrate at 90°C followed by 20-min cool-down at room temperature. After three washes with PBS, the same protocol for mouse immunohistochemistry was followed.

Immunohistochemistry in mouse samples, image acquisition, and quantitative analysis

Animals were anesthetized and perfusedintracardially with 4% PFA in 0.1 M phosphate buffer, pH 7.4. Brains were postfixed in the same solution, cryopreserved in 20% sucrose in 0.1 M phosphatebuffer. Frozen sections were sectioned, mounted for slide imunohistochemistry (15 um) or stored for free-float immunohistochemistry (30 um). After blocking, brain sections were incubated with various primary antibodies, followed by appropriate secondary antibodies (Invitrogen, or Jackson ImmunoResearch). 4′,6-Diamidino-2-phenylindole (DAPI, Vector Laboratories) was used as a nuclear counterstain. For TGFβ-1 and pSMAD2 staining, fluorescence was amplified using Tyramide Signal Amplification kit (Perkin Elmer). Please see supplementary materials for list of antibodies and method for quantification.

Primary OL culture, proliferation and differentiation assays

Enriched oligodendrocyte progenitors were prepared as described[28]. First, a mixed glial culture was prepared by mechanically dissociating the cerebral hemispheres from 1 day old C57BL/6 WT mice and plating on poly-D-lysine-coated flasks in Dulbecco's modified Eagle's medium and Ham's F12 (1:1 vol/vol, hereafter referred to DMEM/F12 medium) (Invitrogen), containing 100 μg/ml gentamicin and supplemented with 4 mg/ml dextrose anhydrous, 3.75 mg/ml HEPES buffer, 2.4 mg/ml sodium bicarbonate and 10% fetal bovine serum (FBS) (Omega Scientific). After 24 hrs the medium was changed and the cells were grown in DMEM/F12 supplemented with insulin (5 μg/ml), human transferrin (50 μg/ml), sodium selenite (30 nM), d-Biotin (10 mM), 0.1% BSA (Sigma Aldrich), 1% horse serum and 1% FBS (Omega Scientific). After 9 days, OL progenitors were purified from the mixed glial culture by the differential shaking and adhesion procedure[29] and allowed to grow on polylysine-coated coverslips in defined culture medium[30]. The purity of culture was 95%, as confirmed by NG2 as well as PDGFRα staining. Please see supplementary materials for list of antibodies and method for assessment.

Primary astrocyte culture and collection of conditioned media

Primary astrocyte cultures were prepared as described[31]. As STAT3-cKO and WT pups were born in the same litter and experimenters were blind to the genotype at the time of tissue collection, individual cultures were obtained from each mouse, resulting in one astrocyte conditioned medium obtained from each mouse pup. Cerebral hemispheres from 0 to 1 day old mice were mechanically dissociated, passed through a 310 um nylon mesh, and plated on poly-D-lysine-coated 100 mm dish containing Eagle's minimum essential medium (MEM) supplemented with 10% FBS, glucose (2 mg/ml), insulin (5 ug/ml), and gentamycin (100 ug/ml). After 3 days, the medium was changed to MEM supplemented with G5 consisted of glucose (4.5 mg/ml), hydrocortisone (10 nM), sodium selenite (30 nM), insulin (5 ug/ml), transferrin (50 ug/ml), biotin (10 ng/ml), bFGF (5 ng/ml) and EGF (10 ng/ml) (Peprotech)[32]. The purity of culture was 98%, as confirmed by GFAP staining as well as exclusion criteria for Olig2 (oligodendrocyte) and CD11b (microglia). Medium was changed

to match the microglia medium DMEM/F12 containing 10% FBS at 11 days in culture, and astrocyte conditioned medium was collected after 72 hrs. For the treatment of microglia, 25% astrocyte conditioned medium supplemented with 75% DMEM/F12 containing 10% FBS was added as described below.

Primary microglia culture and treatment

Primary microglia culture was obtained from the mixed glial culture explained above. At 9 days in culture, microglia were purified by shaking at 200RPM for 1 hr and plated on 24-well plates in DMEM/F12 containing 10% FBS. The purity of culture was at least 92%, confirmed by CD11b and Iba1 staining. Treatment with astrocyte conditioned medium started the following day, in presence of 25 ng/ml LPS to activate microglia. The medium was collected 48 hours later for determination of secreted TGFβ-1 by ELISA.

ELISA

Culture medium was collected from purified astrocyte and microglia cultures before and at the end of treatments specified above and used in sandwich ELISA for TGFβ-1 following manufacturer's protocols (eBioscience).

Statistical analyses

Data are presented as mean ± SEM. Statistical analysis was performed using GraphPad Prism 4.01 software with ANOVA followed by Bonferroni's multiple comparison test, or Friedman test followed by Bonferroni's multiple comparison test. A two-tailed unpaired Student's *t* test was used when two groups were compared. All statistics were considered significant when $P < 0.05$.

Results

Activation of STAT3 pathway in reactive astrogliosis of WMI in human postmortem brains

The presence of reactive gliosis in neonatal WMI has been reported in several histological studies[19, 20, 33]. We confirmed the existence of widespread reactive astrogliosis as well as microgliosis in the white matter in four cases of postmortem brain samples of WMI using the astrocyte marker GFAP and microglia marker Iba1. In all WMI, but not control cases, we observed an intense staining of $GFAP^+$ hypertrophic cells with elongated processes, a hallmark morphology indicative of reactive astrogliosis (Figure 1A, a–b). An abundant $Iba1^+$ microglia with amoeboid morphology were observed in the same areas (Figure 1A, c–d), implying a reactive response to an insult. More detailed examination of reactive astrogliosis revealed that a subset of astrocytes in the white matter showed nuclear localization of phosphorylated STAT3 (pSTAT3), indicating that STAT3 pathway was activated in these cells (Figure 1B). STAT3 activation in astrocytes has been implicated as a principal inducer of the hypertrophic morphology observed in reactive astrogliosis [24], and appears to regulate numerous target genes [34], probably affecting the cellular phenotype. pSTAT3 containing astrocytes were observed in all four cases of WMI regardless of the type of diagnoses (HIE or PVL, see Methods) but none of three age-matched control cases, implicating a molecular signature of reactive astrocytes shared among WMI cases (Table 1).

Paradigm to induce gliosis and WMI in mice

In order to test the specific contribution of glia activation in neonatal WMI, we optimized a mouse model in which astrogliosis and microgliosis along with WMI could be consistently induced in the absence of complicating factors such as gross ischemia or necrosis. To specifically address the effect of gliosis on white matter development, we felt it was important to consider inter-species differences between humans and mice with respect to the

time course of myelin development. The highest risk of WMI in humans occurs at 23–32 gestational weeks, when majority of the white matter is composed of immature, pre-myelinating OL, which are known to be vulnerable to exogenous insults[35, 36]. In mice, this period of white matter development corresponds to the early postnatal period[37], when the great majority of OL-lineage cells express immature markers such as PDGFRα and O4, but not mature markers such as MBP and GSTπ[38]. Indeed, we found that a single subcutaneous injection of lipopolysaccharide (LPS), 10 mg/kg, in the early postnatal period resulted in sustained reactive micro- and astro-gliosis, (Figure 2A and Supplementary Figure 1A) and a subsequent deficit in myelin development (Figure 2C–E), similar to that previously reported inflammation-induced WMI models[40, 41]. Moreover, like in human postmortem tissues, we observed nuclear localization of pSTAT3 in GFAP positive astrocytes starting six hours after peripheral LPS injection (Figure 2B), and lasting up to 5d (later time points shown in Supplementary Figure 1A). Despite activation of STAT3 pathway and the enhanced expression of GFAP, an intermediate filament protein known to increase expression in gliosis (Figure 2A and Supplementary Figure 1A), the expression of another astrocyte marker, S100, a calcium binding protein, was not affected, indicating that LPS had no gross effects on astrocyte development (Supplementary Figure 1B).

In agreement with the notion for time-sensitive risk for white matter injury after various stressors in humans[42], we identified a narrow time window for LPS injection between P1 and P2 that resulted in a significant reduction in MBP (30% – 54% reduction compared to control), whereas beyond P2 there were only marginal non-significant reductions (Figure 2C). These data highlighted the importance of the early and restricted postnatal period P1–2 as a critical window in which the induction of reactive gliosis can disrupt healthy myelination in the mouse forebrain.

Further examination of the immunoreactivity to mature myelin marker MBP revealed that in LPS injected animals, the corpus callosum was less stained and thinner, striatal myelin bundles were smaller, and cortical radiation from the corpus callosum was limited to deep cortical layers (Figure 2D and 2E, e–f) in broad areas spanning from frontal to temporal cortex (Supplementary Figure 1C). Notably, many of LPS injected animals showed enlarged lateral ventricles, a common finding in human patients with WMI (Figure 2D and Supplementary Figure 1C, b–c f–g)[43–46].

In order to determine if the mechanism underlying the hypo-myelinated phenotype was an arrest of OL maturation as implied in studies of human pathological samples[22, 23], we investigated the appearance of maturation-dependent OL lineage markers in the mouse model. Quantification of temporal changes revealed that by 5 days post injection, immunoreactivity for O4, was significantly reduced in large areas of forebrain white matter including corpus callosum and striatum (Figure 2E, c–d and Figure 2F). At this developmental stage, O4 almost exclusively marks OL lineage cells at the preOL stage (beyond progenitor, but pre-differentiated stage) because immunoreactivityies for mature OL markers MBP and GSTπ are barely detectable at this stage. The reduction of O4 at 5 days after LPS was associated with a reduction in mature OL markers MBP and GSTπ in LPS-treated mice at 10 and 15 days post injection, respectively (Figure 2E, e–h and Figure 2F). We did not find evidence for an increased apoptotic death in $Olig2^+$ pan-OL, as assessed by either activated caspase-3 antibody or terminal deoxynucleotidyl transferase dUTP nick end labeling (TUNEL) assay at any of seven time points examined between 2 hr – 20 days (Supplementary Figure 2A shows 3 time points). Delayed appearance of differentiated OL together with the lack of OL death is consistent with a recent clinical study in which myelin staining was altered without apparent OL loss[22, 23], which has led to the proposal that arrested differentiation underlies the observed pathology. Interestingly, the delay in the appearance of mature markers was preceded by a transient increase in the

number of PDGFRα$^+$ OL progenitors (Figure 2E, a–b and Figure 2F), suggesting an accumulation of cells in the white matter at this very early stage. The increased number of progenitors did not appear to be due to enhanced proliferation; in fact, there was a trend for a decrease, which was significant at the 48 hr time point (Supplementary Figure 2B). Finally, numbers of cells labeled with the pan-OL lineage marker Olig2 was not changed by LPS (Fig. 2F), suggesting that the observed changes reflected a shift in cells numbers towards an immature state rather than an overall loss of cells in the OL lineage. In summary, the data suggest that LPS induces an arrest of OL development, without major effects on proliferation or survival.

Over the 20 day time course examined, no evidence of increased neuronal cell death was observed, as assessed by detection of TUNEL staining in NeuN$^+$ cells. Moreover, immunostaining for the pan axonal marker NF160 did not differ between control and LPS-treated mice in callosal bundles where myelin marker was reduced (Supplementary Figure 2C–D), suggesting that the myelin defect was not likely secondary to neuronal or axonal loss. Collectively, these results suggested that a neuroinflammatory insult at this critical period of myelination is sufficient to induce a deficit in myelin development, through a mechanism of impaired production and/or arrested differentiation of OL progenitors.

Role of STAT-3 mediated reactive astrogliosis in white matter injury

As discussed above, nuclear localization of pSTAT3 was detected in GFAP positive cells in LPS-treated mice (Figure 2B and Supplementary Figure 1A), similar to that observed in clinical WMI cases (Figure 1B). To investigate the role of STAT3-mediated induction of reactive astrogliosis in neonatal WMI, we used mice harboring an astrocyte-specific deletion of STAT3 gene (STAT3-cKO mice). The transgenic Cre driver mouse line used a 15 kb mouse GFAP promoter cassette, and targets astrocytes that express high levels of GFAP, postnatal GFAP$^+$ neural stems cells, but not embryonic radial glia (described in[47]). By immunohistochemistry, the expression of a reporter protein β-galactosidase driven by a floxed ROSA26 promoter[27] in mice harboring the same GFAP-Cre cassette was found to be almost undetectable in the forebrain white matter of non-LPS injected animals at P2 (Supplementary Figure 3A, a–c), confirming the limited Cre-mediated excision activity at this time point in the absence of LPS. On the other hand, when astrocytes become hypertrophic and upregulate GFAP expression in response to LPS, β-gal was specifically detected in GFAP$^+$ astrocytes (Supplementary Figure 3A, d–f). These data suggested that the GFAP-Cre line spared endogenous astrocytes at the time of LPS injection, and induced Cre-mediated recombination in response to the inflammatory insult.

Untreated STAT3-cKO mice showed a normal time course of induction of OL maturation markers, tested at P2 (PDGFRα for OL progenitors), P7 (O4 for immature OL), and at P12 (MBP for mature OL) (Supplementary Figure 3B, a–f). The nuclear localization of pSTAT3 observed in numerous astrocytes of STAT3-WT mice after LPS injection was abolished in STAT3-cKO mice (Figure 3A), confirming the integrity of the STAT3 excision in reactive astrocytes. The functional inactivation of the STAT3 pathway was demonstrated by the fact that STAT3-cKO mice failed to exhibit the hypertrophic reactive astrocyte morphology observed in STAT3-WT littermates (Figure 3A–B) even in the presence of an inflammatory insult. This was expected because the STAT3 pathway is reported to be a critical inducer of astrocyte hypertrophy[24].

In order to test the effects of attenuated STAT3 signaling in reactive astrocytes on myelin development, MBP, a myelin protein expressed primarily in mature OL was quantified. The decreased MBP expression induced by LPS in STAT3-WT mice was more pronounced in STAT3-cKO mice at 10 days post LPS, as determined by Western blot and immunohistochemistry (Figure 3C–D). Moreover, there was no evidence for increased

TUNEL-dependent cell death in OL (Supplementary Figure 4A), suggesting that the exacerbated myelin defect in STAT3-cKO was not associated with appreciable OL apoptosis. Because GFAP is also strongly expressed in postnatal stem cells that potentially generate OL[48], we addressed the possibility that STAT3-deletion in GFAP$^+$ neural stem cells diminished the production of OL. To do this we followed the fate of cells undergoing Cre-mediate recombination and their progeny using the aforementioned β-gal reporter driven by the same GFAP-Cre driver. Only 1–2% of mature (GSTπ^+) OL appearing at this stage expressed β-galactosidase in the basal state, and the LPS injection did not alter this percentage (Supplementary Figure 4B) at P20. These results indicated that the contribution of postnatal GFAP$^+$ stem cells to the OL lineage is small at this stage, and not significantly altered by LPS injection. Thus, a diminished production of OL from GFAP$^+$ neural stem cells is unlikely to play a role in the exacerbated myelin injury.

TGFβ-1 as a possible mediator of inflammatory injury controlled by astrocytic STAT3

In order to investigate the mechanism by which astrocytic STAT3 pathway imposed a non-cell autonomous effect on the process of myelination, we screened for candidate factors with aberrant temporal production in STAT3-cKO brain after LPS injection. TGFβ-1 was found to fulfill the criteria as a factor whose over-expression might delay OL maturation. TGFβ-1, a BMP family cytokine, signals through transcription factors SMAD2 and SMAD3, distinct from those induced by BMPs (SMAD1, 5, and 8). TGFβ-1 has been shown to affect differentiation of a broad range of cell types outside the CNS[49–52], but its functions on oligodendrocyte development are unknown. Interestingly, TGFβ-1 expression in the postnatal brain of untreated wild type mice was strongly developmentally regulated, being the highest at the neonatal stage (P2), then decreasing and becoming nearly undetectable by immunohistochemistry by P12 (Figure 4A, a–c). A similar age-dependent decrease was observed in gene expression levels (Figure 4A, right panel). Importantly, essentially all detectable TGFβ-1 immunoreactivity was colocalized to CD68$^+$ microglia at each of the time points examined, whereas no detectable colocalization was found in GFAP$^+$ astrocytes (Figure 4A, d–i). After LPS injection, TGFβ-1 expression was significantly increased in LPS-injected mice compared to control-injected mice in broad regions of forebrain, and increased even further in mice with the conditional STAT3 deletion (Figure 4B). Double immunostaining revealed that regardless of genotype and time point, TGFβ-1 expression was exclusively colocalized to microglia (Figure 4B), suggesting microglia as the primary source of TGFβ-1.

If TGFβ-1 indeed acted on nearby OL precursors to regulate their development, it might be expected that the downstream TGFβ-1 signal transducer, phosphorylated SMAD2 (pSMAD2) would be detectable in cells in the OL lineage at early postnatal stages (when TGFβ-1 expression is high). Moreover, pSMAD2 levels are expected to be increased after LPS administration, due to its apparent induction of TGFβ-1 expression. We confirmed the expression of pSMAD2 in Olig2$^+$ cells in non-injected WT mice at P3, which decreased as animals aged to P12 (data not shown). Consistent with the hypothesis, we found that the proportion of pSMAD2$^+$/Olig2$^+$ double positive cells was significantly increased by LPS injection, and further increased in LPS-treated STAT3-cKO mice beyond observed in similarly treated STAT3-WT mice (Figure 4C–D).

The observation that LPS-induced TGFβ-1 expression in microglia was differentially affected in STAT3-cKO vs. WT mice raised the question of how astrocyte-specific differences in STAT3 activity could mediate this altered microglial phenotype. In order to test the ability of astrocytes to directly control microglial TGFβ-1 expression, we purified astrocytes from STAT3-cKO and STAT3-WT littermates (therefore astrocytes were either KO or WT in STAT3) and collected their conditioned media. We confirmed constitutive basal expression of pSTAT3 in cultured WT astrocytes (Supplementary figure 5) as

suggested in literature[53]. Media from these cells, containing secreted factors from astrocytes, were added to purified primary microglia obtained from C57BL/6 WT mice, which had not been affected by genetic manipulation during their development, and the secretion of TGFβ-1 was measured by ELISA. Microglia cultured alone were found to secrete 0.761±0.042 ng/ml TGFβ-1 into their medium. However, when they were cultured in presence of astrocyte conditioned medium obtained from STAT3-WT astrocytes, TGFβ-1 in the medium was significantly reduced (Figure 4E), suggesting that astrocytes secrete factor(s) with the capacity to limit TGFβ-1 production by microglia. On the other hand, when microglia were treated with medium from STAT3-KO astrocytes, levels of TGFβ-1 were not significantly reduced, and remained at a similar level to microglia cultured alone (Figure 4E). The source of TGFβ-1 is most likely microglia, because astrocyte conditioned media did not contain live cells and the purity of microglia cultures was >92%. In addition, the contribution of TGFβ-1 secreted by astrocytes before addition to microglia was found to be low and similar between STAT3-cKO and STAT3-WT (0.072±0.047 ng/ml in KO, 0.065±0.072 ng/ml in WT). These results suggested that STAT3 signaling in astrocytes regulates the secretion of factors to limit the production of TGFβ-1 from microglia in vitro. Moreover, the results raised the possibility that astrocytic STAT3 signaling might serve as a cell non-autonomous mechanism to inhibit the microglial production of TGFβ-1 during an inflammatory insult, when STAT3 pathway becomes activated. On the other hand, exogenously applied TGFβ-1 did not induce STAT3 pathway activity in astrocytes, suggesting that activation of STAT3 signaling in astrocytes did not occur as a result of overexpressed TGFβ-1 (Supplementary Figure 7).

TGFβ-1 directly inhibits OL differentiation in culture

The fact that that the disappearance of TGFβ-1 expression in untreated wild type mice coincided with the appearance of mature OL marker MBP, and that the disappearance was delayed under conditions of excess TGFβ-1 in association with myelin injury (see Figure 4B) suggested that microglial TGFβ-1 might function as a molecular “brake” in normal OL differentiation, and might further delay OL differentiation after induction of astrogliosis. In this respect, the disappearance of TGFβ-1 expression could be important trigger for the commencement of myelin development, and that its disappearance needs to be carefully timed to result in properly-timed myelination. To test whether TGFβ-1 has the capacity to act directly on OL to regulate their development, we prepared cultures of purified OL progenitors from WT mice, and investigated their development in presence and absence of TGFβ-1. As assessed by Western blot, there was an upregulation of pSMAD2 expression within 2 hrs of TGFβ-1 application, confirming their ability to respond to exogenous TGFβ-1 (Figure 5A). The development of the OL progenitors proceeds with proliferation and differentiation, so to study these processes independently, we examined the effects of TGFβ-1 under separate conditions. In conditions under which the proliferation of OL progenitors is maintained (i.e., in media containing mitogens PDGF-A and bFGF for 48 hours), proliferation, as determined by bromo-deoxyuridine (BrdU) incorporation after a 24 hr pulse was decreased by TGFβ-1 in a dose dependent manner. Similar results were obtained using another mitotic marker phosphorylated histone H3 (Figure 5B). Under conditions where OL progenitors were allowed to differentiate for 48 hr, TGFβ-1 induced a dose-dependent decrease in the proportion of cells that expressed mature markers CC1, O1, and MBP, and an increase in cells that retained immature OL markers PDGFRα, Sox9 and Sox2 (Figure 5C). Additionally, delayed differentiation of OL progenitors was confirmed by assessing the morphological complexity, which yielded supporting results that TGFβ-1 treatment dose-dependently limited the extension of processes, maintaining the cells in immature morphology (Supplementary Figure 6).

Next, to test the involvement of TGFβ-1 signaling on myelination in vivo, a selective inhibitor of the signaling pathway, SB431542 (Cayman Chemical), was administered during normal myeilin development as well as during LPS-induced WMI paradigm. SB431542 inhibits the kinase activity of TGFβ specific receptor ALK5 thereby blocking SMAD2 signaling but spares SMAD1/5/8 signaling used by BMPs[54]. Its efficacy has been shown in vivo in adult mouse models of various diseases[55–57], and in neonatal mice, was found to be effective in reducing the phorphosrylation of SMAD2 in the brain when administered intraperitoneally at P2 (Figure 5D). The administration of SB431542 at P2 during normal development induced a small, non-significant increase in mature myelin protein MBP. Importantly, upon LPS injection, SB431542 was found to partially rescue the reduction of MBP by about 50% (Figure 5E), suggesting a critical involvement of sustained SMAD2 activity in the delayed myelin development observed in LPS injected mice. Collectively, these in vitro and in vivo results demonstrated that prolonged activation of TGFβ-1 signaling may be a key pathological modulator in neonatal brain development. The observation that the reduction of TGFβ-1 expression was delayed after LPS injection and that microglia were the only detectable source of TGFβ-1 at all time points (see Figure 4B), together with the finding that expression levels of TGFβ-1 were affected by astrocyte-specific STAT3 signaling, suggests a non-cell autonomous mechanism involving at least three different cell types, whereby reactive astrocytes alters the microglial secretion of TGFβ-1, which in turn acts on OL progenitors to alter their development.

Human postmortem brain samples of preterm infants with non-focal WMI express high levels of TGFβ-1 in microglia

To determine if overt TGFβ-1 expression in microglia is also a characteristic of human cases of WMI, we stained samples of the human postmortem cases in Table 1 with antibodies against human TGFβ-1 and the microglia marker Iba1. In all cases of WMI, there was abundant expression of TGFβ-1 in the white matter. Moreover, a majority of the TGFβ-1 staining localized to Iba1 positive cells, demonstrating the microglial expression of TGFβ-1 (Figure 6). Notably, microglia containing TGFβ-1 showed hypertrophic, amoeboid morphology, indicative of an activated phenotype. These studies indicate that TGFβ-1 signaling might represent a therapeutic target to limit WMI in babies at risk for this pathology.

Discussion

Reactive astrogliosis is a hallmark of neonatal brain injury and many other pathologies of the CNS. Despite this commonality, its beneficial vs. harmful consequences in various contexts are not well understood, and cell non-autonomous effects of astrogliosis on neonatal brain development have never been demonstrated. Although inflammatory insults and hypoxic-ischemic events are considered the main causal factors for neonatal WMI, the multifactorial nature of the pathology has limited the advances of our mechanistic understanding. In this regard, pathological studies on hypoxic-ischemia cases generally show concurrent micro- and astro-gliosis, making it difficult to dissociate the sequence of key factors leading to the white matter pathology. In the current model, we attempted to study the reactive glia component of neonatal WMI in relative isolation, and therefore optimized an inflammation to consistently induce gliosis in mice at a time corresponding to the heightened vulnerability to WMI in humans. We found that a single peripherally-administered dose of LPS was sufficient to induce micro-and astro-gliosis and WMI injury in mice in a pattern consistent with that observed in human postmortem cases. This protocol, along with genetically-engineered mice were then used to probe the complex nature of neonatal brain injury. Importantly, the studies revealed a protective role of astrocytes, and

led to the identification of a candidate pathway for disease protection involving modulation of the TGFβ-1 signaling pathway.

Our data in human postmortem tissues of neonatal WMI samples demonstrated that the STAT3 pathway was commonly active in hypertrophic astrocytes, so the potential consequences of STAT3-mediated astrogliosis were investigated in our model using conditional knockout mice. The STAT3 pathway has been demonstrated to be a mediator of reactive astrogliosis, particularly with respect to GFAP upregulation, hypertrophic morphology, and scar formation [24]. By manipulating the STAT3 gene in astrocytes, we demonstrated a protective role of reactive astrocytes in limiting myelin injury. An investigation of potential mechanisms revealed that aberrant TGFβ-1 in microglia might be a key factor in this pathology. In this regard, TGFβ-1 was found to be tightly regulated during development in healthy mice, and was detected exclusively in microglia. Moreover, it was suggested that excess TGFβ-1 had a direct action on developing OL, as evidenced by the fact that higher levels of the signal transducer pSMAD2 were observed in OL lineage cells in vivo under conditions of high TGFβ-1, and that TGFβ-1 inhibited the maturation of purified OL progenitors in culture. The that fact that pharmacological inhibition of pSMAD2 pathway partially reversed the inflammation-induced delayed myelin development in vivo suggest that TGFβ-1 signaling might be a therapeutic target for limiting myelin defects in infants at risk for WMI. However, it must be cautioned that the ability of TGFβ-1 blockade to diminish perinatal white matter injury may be model dependent. For example, other factors, including cytokines IL-6, IL-10, ciliary neurotrophic factor (CNTF), and leukemia inhibitory factor (LIF) in addition to LPS can activate STAT3 pathway in astrocytes, and it is uncertain if they would trigger a similar STAT3-dependent induction of TGFβ-1. In any case, the current study highlights a new role of TGFβ-1 in neonatal brain development, whose dysregulation may mediate pathology associated with a type of WMI.

Interestingly, whereas we showed TGFβ-1 was expressed primarily in microglia of postmortem WMI samples, and exclusively in microglia in the normal and inflamed neonatal mouse brain, TGFβ-1 immunoreactivity has been demonstrated in both macrophages and reactive astrocytes in multiple sclerosis (MS) lesions[58]. Zhang et al. recently proposed an alternative mechanism in which astrocytes expressing TGFβ-1 in MS lesions was hypothesized to induce Jagged1/Notch1 signaling in OL, thereby inhibiting their differentiation[59]. Being a secreted molecule, TGFβ-1 can be secreted by a variety of cellular sources and may potentially act on multiple cell types with appropriate receptors. However, as discussed, we did not observe expression of TGFβ-1 in astrocytes in the mouse model, and the great majority of cells expressing TGFβ-1 in human postmortem tissues were Iba^+ microglia. On the other hand, in the developing mouse brain, Jagged1 expression was found exclusively in callosal axons in discrete locations and rapidly became undetectable during the examined postnatal period (data not shown). Based on these observations, it is unlikely that the Jagged1 expression by reactive astrocytes contributed significantly to the broadly affected pathology we reported in the neonatal mouse model used here.

Another potential mechanism is suggested by the fact that astrocytes are known to secrete cytokines including LIF[60] and CNTF[61] which promote survival and maturation of OL. In addition, reactive astrocytes are known to express factors such as FGF2[62] and hyaluronan[63] that are inhibitory for OL differentiation. Of those, we examined expression levels of LIF in our model and found that it was mildly upregulated by LPS, but was not regulated in astrocytic STAT3-dependent manner (data not shown). How other molecules are regulated in the context of inflammatory insult in the neonatal brain requires further examination.

Why should an inhibitory factor for myelination be highly expressed in newborn brain, at the time when myelin is developing? One potential explanation is that OL progenitors must

be maintained at an immature stage until neuronal connections are fully established and/or until other developmental processes are complete. The disruption of such a carefully-timed process by astrogliosis could presumably have pathological effects on subsequent CNS function. Notably, microglial expression of TGFβ-1, as well as nuclear pSTAT3 in reactive astrocytes was observed in the white matter of human neonatal WMI examined here. Using cell culture system, we demonstrated that astrocyte-derived factors (obtained from conditioned media from WT vs. STAT3-deficient astrocytes) had the capacity to differentially regulate TGFβ-1 secretion by cultured microglia. Although the identification of that factor remains unknown, Sarafian et al. recently reported microarray data on STAT3 WT and deficient astrocytes, which may suggest potential candidate genes[53].

In summary, the clinical evidence presented along with the findings reported here in mouse and tissue culture models suggest that STAT3-mediated reactive astrocytes attempt to protect myelin development against neuroinflammation by constraining microglial TGFβ-1 expression in cell non-autonomous manner. These observations imply a potential benefit of promoting STAT3 pathway activation during inflammatory insult. Collectively, the results presented here support the concept that process of healthy myelination involves intricate and timed communications among multiple glial cell types, and that the temporally-regulated communication can be dysregulated by reactive astrogliosis during a critical time, leading to impairment in myelin development.

Supplementary Material

Refer to Web version on PubMed Central for supplementary material.

Acknowledgments

This work was supported by the grants from the US National Institute of Health to J.A.W. (NS070580, HD057557), to J.d.V. (HD04612), and to M.V.S. (NS057624), and by the University of California Multicampus Research Programs and Initiatives (E.J.H., H.V.V.)

References

1. Back SA. Perinatal white matter injury: the changing spectrum of pathology and emerging insights into pathogenetic mechanisms. Ment Retard Dev Disabil Res Rev. 2006; 12:129–140. [PubMed: 16807910]
2. Volpe JJ, Kinney HC, Jensen FE, Rosenberg PA. Reprint of “The developing oligodendrocyte: key cellular target in brain injury in the premature infant”. Int J Dev Neurosci. 2011
3. Silbereis JC, Huang EJ, Back SA, Rowitch DH. Towards improved animal models of neonatal white matter injury associated with cerebral palsy. Dis Model Mech. 2010; 3:678–688. [PubMed: 21030421]
4. Dyet LE, Kennea N, Counsell SJ, et al. Natural history of brain lesions in extremely preterm infants studied with serial magnetic resonance imaging from birth and neurodevelopmental assessment. Pediatrics. 2006; 118:536–548. [PubMed: 16882805]
5. Rezaie P, Dean A. Periventricular leukomalacia, inflammation and white matter lesions within the developing nervous system. Neuropathology. 2002; 22:106–132. [PubMed: 12416551]
6. Blumenthal I. Periventricular leucomalacia: a review. Eur J Pediatr. 2004; 163:435–442. [PubMed: 15179510]
7. Deng W, Pleasure J, Pleasure D. Progress in periventricular leukomalacia. Arch Neurol. 2008; 65:1291–1295. [PubMed: 18852342]
8. Bhutta AT, Cleves MA, Casey PH, et al. Cognitive and behavioral outcomes of school-aged children who were born preterm: a meta-analysis. JAMA. 2002; 288:728–737. [PubMed: 12169077]

9. Constable RT, Ment LR, Vohr BR, et al. Prematurely born children demonstrate white matter microstructural differences at 12 years of age, relative to term control subjects: an investigation of group and gender effects. Pediatrics. 2008; 121:306–316. [PubMed: 18245422]
10. Skranes J, Vangberg TR, Kulseng S, et al. Clinical findings and white matter abnormalities seen on diffusion tensor imaging in adolescents with very low birth weight. Brain. 2007; 130:654–666. [PubMed: 17347255]
11. Dammann O, Leviton A. Inflammatory brain damage in preterm newborns--dry numbers, wet lab, and causal inferences. Early Hum Dev. 2004; 79:1–15. [PubMed: 15282118]
12. Leviton A, Paneth N, Reuss ML, et al. Maternal infection, fetal inflammatory response, and brain damage in very low birth weight infants. Developmental Epidemiology Network Investigators. Pediatr Res. 1999; 46:566–575. [PubMed: 10541320]
13. Chau V, Brant R, Poskitt KJ, et al. Postnatal infection is associated with widespread abnormalities of brain development in premature newborns. Pediatr Res. 71:274–279. [PubMed: 22278180]
14. Nelson KB, Grether JK, Dambrosia JM, et al. Neonatal cytokines and cerebral palsy in very preterm infants. Pediatr Res. 2003; 53:600–607. [PubMed: 12612192]
15. Wu YW. Systematic review of chorioamnionitis and cerebral palsy. Ment Retard Dev Disabil Res Rev. 2002; 8:25–29. [PubMed: 11921383]
16. Yoon BH, Romero R, Yang SH, et al. Interleukin-6 concentrations in umbilical cord plasma are elevated in neonates with white matter lesions associated with periventricular leukomalacia. Am J Obstet Gynecol. 1996; 174:1433–1440. [PubMed: 9065108]
17. Roessmann U, Gambetti P. Pathological reaction of astrocytes in perinatal brain injury. Immunohistochemical study. Acta Neuropathol. 1986; 70:302–307. [PubMed: 3532687]
18. Hirayama A, Okoshi Y, Hachiya Y, et al. Early immunohistochemical detection of axonal damage and glial activation in extremely immature brains with periventricular leukomalacia. Clin Neuropathol. 2001; 20:87–91. [PubMed: 11327303]
19. Deguchi K, Oguchi K, Takashima S. Characteristic neuropathology of leukomalacia in extremely low birth weight infants. Pediatr Neurol. 1997; 16:296–300. [PubMed: 9258961]
20. Andiman SE, Haynes RL, Trachtenberg FL, et al. The cerebral cortex overlying periventricular leukomalacia: analysis of pyramidal neurons. Brain Pathol. 2010; 20:803–814. [PubMed: 20331617]
21. Sofroniew MV, Vinters HV. Astrocytes: biology and pathology. Acta Neuropathol. 2010; 119:7–35. [PubMed: 20012068]
22. Billiards SS, Haynes RL, Folkerth RD, et al. Myelin abnormalities without oligodendrocyte loss in periventricular leukomalacia. Brain Pathol. 2008; 18:153–163. [PubMed: 18177464]
23. Buser JR, Maire J, Riddle A, et al. Arrested preoligodendrocyte maturation contributes to myelination failure in premature infants. Ann Neurol. 71:93–109. [PubMed: 22275256]
24. Herrmann JE, Imura T, Song B, et al. STAT3 is a critical regulator of astrogliosis and scar formation after spinal cord injury. J Neurosci. 2008; 28:7231–7243. [PubMed: 18614693]
25. Garcia AD, Doan NB, Imura T, et al. GFAP-expressing progenitors are the principal source of constitutive neurogenesis in adult mouse forebrain. Nat Neurosci. 2004; 7:1233–1241. [PubMed: 15494728]
26. Takeda K, Kaisho T, Yoshida N, et al. Stat3 activation is responsible for IL-6-dependent T cell proliferation through preventing apoptosis: generation and characterization of T cell-specific Stat3-deficient mice. J Immunol. 1998; 161:4652–4660. [PubMed: 9794394]
27. Soriano P. Generalized lacZ expression with the ROSA26 Cre reporter strain. Nat Genet. 1999; 21:70–71. [PubMed: 9916792]
28. Amur-Umarjee S, Phan T, Campagnoni AT. Myelin basic protein mRNA translocation in oligodendrocytes is inhibited by astrocytes in vitro. J Neurosci res. 1993; 36:99–110. [PubMed: 7693963]
29. Suzumura A, Bhat S, Eccleston PA, et al. The isolation and long-term culture of oligodendrocytes from newborn mouse brain. Brain Res. 1984; 324:379–383. [PubMed: 6397235]
30. Agresti C, D'Urso D, Levi G. Reversible inhibitory effects of interferon-gamma and tumour necrosis factor-alpha on oligodendroglial lineage cell proliferation and differentiation in vitro. Eur J Neurosci. 1996; 8:1106–1116. [PubMed: 8752580]

31. Yoshida T, Takeuchi M. Primary culture and cryopreservation of mouse astrocytes under serum-free conditions. Cytotechnology. 1991; 5:99–106. [PubMed: 1367159]
32. Michler-Stuke A, Wolff J, Bottenstein JE. Factors influencing astrocyte growth and development in defined media. Int J Devl Neuroscience. 1984; 2:575–584.
33. Haynes RL, Folkerth RD, Keefe RJ, et al. Nitrosative and oxidative injury to premyelinating oligodendrocytes in periventricular leukomalacia. J Neuropathol Exp Neurol. 2003; 62:441–450. [PubMed: 12769184]
34. Sofroniew MV. Molecular dissection of reactive astrogliosis and glial scar formation. Trens Neurosci. 2009; 32:638–647.
35. Volpe JJ. Neurobiology of periventricular leukomalacia in the premature infant. Pediatr Res. 2001; 50:553–562. [PubMed: 11641446]
36. Back SA, Riddle A, McClure MM. Maturation-dependent vulnerability of perinatal white matter in premature birth. Stroke. 2007; 38:724–730. [PubMed: 17261726]
37. Craig A, Ling Luo N, Beardsley DJ, et al. Quantitative analysis of perinatal rodent oligodendrocyte lineage progression and its correlation with human. Exp Neurol. 2003; 181:231–240. [PubMed: 12781996]
38. Hasegawa M, Houdou S, Mito T, et al. Development of myelination in the human fetal and infant cerebrum: a myelin basic protein immunohistochemical study. Brain Dev. 1992; 14:1–6. [PubMed: 1375444]
39. Paintlia MK, Paintlia AS, Contreras MA, et al. Lipopolysaccharide-induced peroxisomal dysfunction exacerbates cerebral white matter injury: attenuation by N-acetyl cysteine. Exp Neurol. 2008; 210:560–576. [PubMed: 18291369]
40. Hagberg H, Peebles D, Mallard C. Models of white matter injury: comparison of infectious, hypoxic-ischemic, and excitotoxic insults. Ment Retard Dev Disabil Res Rev. 2002; 8:30–38. [PubMed: 11921384]
41. Choi EK, Park D, Kim TK, et al. Animal models of periventricular leukomalacia. Lab Anim Res. 2011; 27:77–84. [PubMed: 21826166]
42. Ferriero DM, Miller SP. Imaging selective vulnerability in the developing nervous system. J Anat. 2010; 217:429–435. [PubMed: 20408904]
43. Skranes J, Vangberg TR, Kulseng S, et al. Clinical findings and white matter abnormalities seen on diffusion tensor imaging in adolescents with very low birth weight. Brain. 2007; 130:654–666. [PubMed: 17347255]
44. Nguyen The Tich S, Anderson PJ, Shimony JS, et al. A novel quantitative simple brain metric using MR imaging for preterm infants. AJNR Am J Neuroradiol. 2009; 30:125–131. [PubMed: 18832662]
45. Fu J, Xue X, Chen L, et al. Studies on the value of diffusion-weighted MR imaging in the early prediction of periventricular leukomalacia. J Neuroimaging. 2009; 19:13–18. [PubMed: 18393955]
46. Nagy Z, Jonsson B. Cerebral MRI findings in a cohort of ex-preterm and control adolescents. Acta Paediatr. 2009; 98:996–1001. [PubMed: 19469719]
47. Sofroniew MV. Transgenic techniques for cell ablation or molecular deletion to investigate functions of astrocytes and other GFAP-expressing cell types. Methods Mol Biol. 814:531–544. [PubMed: 22144330]
48. Menn B, Garcia-Verdugo JM, Yaschine C, et al. Origin of oligodendrocytes in the subventricular zone of the adult brain. J Neurosci. 2006; 26:7907–7918. [PubMed: 16870736]
49. Pietenpol JA, Stein RW, Moran E, et al. TGF-beta 1 inhibition of c-myc transcription and growth in keratinocytes is abrogated by viral transforming proteins with pRB binding domains. Cell. 1990; 61:777–785. [PubMed: 2140528]
50. Defacque H, Piquemal D, Basset A, et al. Transforming growth factor-beta1 is an autocrine mediator of U937 cell growth arrest and differentiation induced by vitamin D3 and retinoids. J Cell Physiol. 1999; 178:109–119. [PubMed: 9886497]
51. Yang X, Chen L, Xu X, et al. TGF-beta/Smad3 signals repress chondrocyte hypertrophic differentiation and are required for maintaining articular cartilage. J Cell Biol. 2001; 153:35–46. [PubMed: 11285272]

52. Marone M, Scambia G, Bonanno G, et al. Transforming growth factor-beta1 transcriptionally activates CD34 and prevents induced differentiation of TF-1 cells in the absence of any cell-cycle effects. Leukemia. 2002; 16:94–105. [PubMed: 11840268]
53. Sarafian TA, Montes C, Imura T, et al. Disruption of astrocyte STAT3 signaling decreases mitochondrial function and increases oxidative stress in vitro. PLoS One. 5:e9532. [PubMed: 20224768]
54. Inman GJ, Nicolas FJ, Callahan JF, et al. SB-431542 is a potent and specific inhibitor of transforming growth factor-beta superfamily type I activin receptor-like kinase (ALK) receptors ALK4, ALK5, and ALK7. Mol Pharmacol. 2002; 62:65–74. [PubMed: 12065756]
55. Ronaldson PT, Demarco KM, Sanchez-Covarrubias L, et al. Transforming growth factor-beta signaling alters substrate permeability and tight junction protein expression at the blood-brain barrier during inflammatory pain. J Cereb Blood Flow Metab. 2009; 29:1084–1098. [PubMed: 19319146]
56. Waghabi MC, de Souza EM, de Oliveira GM, et al. Pharmacological inhibition of transforming growth factor beta signaling decreases infection and prevents heart damage in acute Chagas' disease. Antimicrob Agents Chemother. 2009; 53:4694–4701. [PubMed: 19738024]
57. Lonardo E, Hermann PC, Mueller MT, et al. Nodal/Activin signaling drives self-renewal and tumorigenicity of pancreatic cancer stem cells and provides a target for combined drug therapy. Cell Stem Cell. 9:433–446. [PubMed: 22056140]
58. De Groot CJ, Montagne L, Barten AD, et al. Expression of transforming growth factor (TGF)-beta1, -beta2, and -beta3 isoforms and TGF-beta type I and type II receptors in multiple sclerosis lesions and human adult astrocyte cultures. J Neuropathol Exp Neurol. 1999; 58:174–187. [PubMed: 10029100]
59. Zhang Y, Zhang J, Navrazhina K, et al. TGFbeta1 induces Jagged1 expression in astrocytes via ALK5 and Smad3 and regulates the balance between oligodendrocyte progenitor proliferation and differentiation. Glia. 2010; 58:964–974. [PubMed: 20169621]
60. Ishibashi T, Dakin KA, Stevens B, et al. Astrocytes promote myelination in response to electrical impulses. Neuron. 2006; 49:823–832. [PubMed: 16543131]
61. Albrecht PJ, Murtie JC, Ness JK, et al. Astrocytes produce CNTF during the remyelination phase of viral-induced spinal cord demyelination to stimulate FGF-2 production. Neurobiol Dis. 2003; 13:89–101. [PubMed: 12828933]
62. Messersmith DJ, Murtie JC, Le TQ, et al. Fibroblast growth factor 2 (FGF2) and FGF receptor expression in an experimental demyelinating disease with extensive remyelination. J Neurosci Res. 2000; 62:241–256. [PubMed: 11020217]
63. Back SA, Tuohy TM, Chen H, et al. Hyaluronan accumulates in demyelinated lesions and inhibits oligodendrocyte progenitor maturation. Nat Med. 2005; 11:966–972. [PubMed: 16086023]
64. Yanagisawa M, Nakashima K, Arakawa H, et al. Astrocyte differentiation of fetal neuroepithelial cells by interleukin-11 via activation of a common cytokine signal transducer, gp130, and a transcription factor, STAT3. J Neurochem. 2000; 74:1498–1504. [PubMed: 10737606]

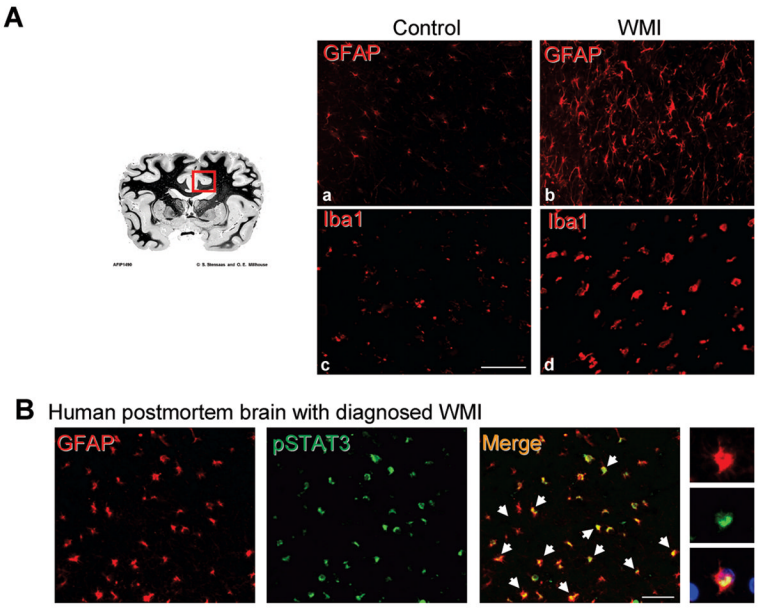

Figure 1. Human postmortem WMI show reactive gliosis and activation of STAT3 pathway within the white matter

(A) Reactive gliosis confirmed by GFAP (astrocyte, a–b) and Iba1 (microglia, c–d) staining of the white matter underlying cingulate gyrus (a boxed area) within a human postmortem WMI brain is shown (case 2 shown, also see table 1). Extensive processes in GFAP as well as hypertrophic morphology in Iba1 indicated presence of gliosis. Brain image on left was obtained from the collection of images of the Armed Forces Institute of Pathology Collection and the University of Utah. Scale bar = 100 um. **(B)** Activation of STAT3 pathway, as evidenced by nuclear pSTAT3, is present in astrocytes within human WMI brains. Four cases of human WMI, (case 2 shown), were stained for GFAP (astrocytes) and pSTAT3. Nuclear pSTAT3 was observed in wide areas of white matter in human WMI brain; a subset colocalized to $GFAP^+$ astrocytes. Also see table 1. Scale bar = 100 um.

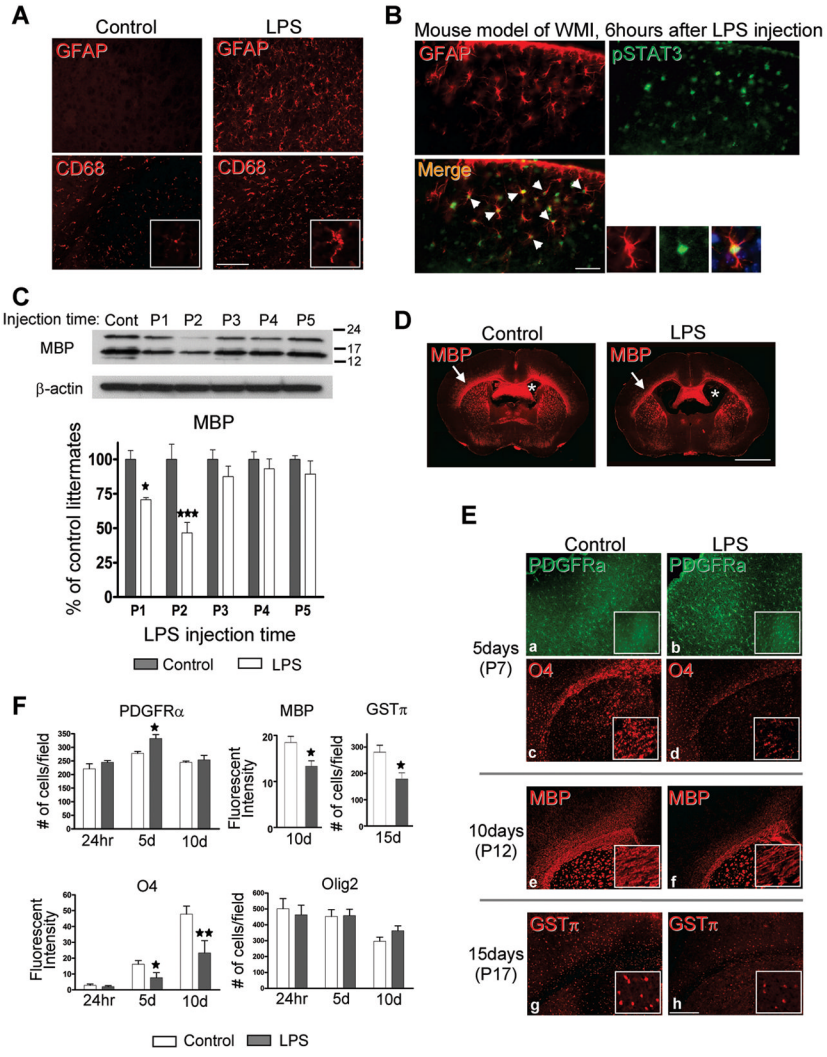

Figure 2. Reactive gliotic response followed by reduced myelinogenesis in the postnatal mouse brain after peripheral administration of lipopolysaccharide (LPS)

(A) Astrocyte and microglia activation was observed within 24 hours after LPS in broad areas of the white matter (striatum shown). Changes observed included 1) increased intensity of immunofluorescence, 2) conversion to a hypertrophic morphology, and 3) increased number of detected microglia. Scale bar = 200 um. **(B)** Phosphorylated STAT3 localized in nuclei of GFAP$^+$ astrocytes is observed starting 6 hrs after LPS injection (cortex shown). Scale bar = 200 um; right panels show higher magnification, with the nuclear DAPI stains (blue). **(C)** Reduction of MBP levels as a function of postnatal day of injection. LPS was injected at different time points during postnatal period (P1 to P5) and mature myelin protein MBP was measured at P20 by Western blot. LPS injections at P1 and P2 were the only time points that resulted in significant MBP reduction. N=5–8 in each time point. P-values represent * <0.05, ***<0.001. **(D)** Immunohistochemistry for myelin protein MBP revealed that LPS caused a reduction in MBP in widespread regions at 10 days post injection. Notable reduction in MBP immunofluorescence was observed in white matter regions such as corpus callosum (arrows) and striatum as well as in gray matter regions (cortex, thalamus). Enlarged lateral ventricles (asterisks) was a common characteristic in LPS injected mice. Scale bar = 2 mm. **(E)** Evidence for an LPS-induced defect in myelin development. Whereas staining for the OL progenitor marker PDGFRα$^+$ (a–b) revealed a

transient increase at 5 days after LPS injection (P7), immature OL marker O4 (c–d) was reduced. A mature OL marker MBP (e–f) was significantly decreased in mice at 10 days after injection (P12). By 15 days after injection (P17), the number of even more mature GSTπ^+ OL (g–h) was reduced in the same areas of LPS-treated mice (e–f, striatal counts shown). N=4–6 in each group. Scale bar = 500 um. P-values represent * <0.05. **(F)** Quantification of time course dependent changes in OL lineage cells. OL progenitors (PDGFRα^+), immature/mature OL ($O4^+$), mature (MBP^+ and GSTπ^+), total OL ($Olig2^+$) were counted (when individual cells were discrete) or measured in fluorescence (when cells could not be separated) from stained sections. Whereas total number of OL (Olig2) was unchanged throughout the time course, a transient increase in OL progenitors (PDGFRα) and reduction in mature OL (MBP and GSTπ) were observed. P-values represent * <0.05, **<0.01.

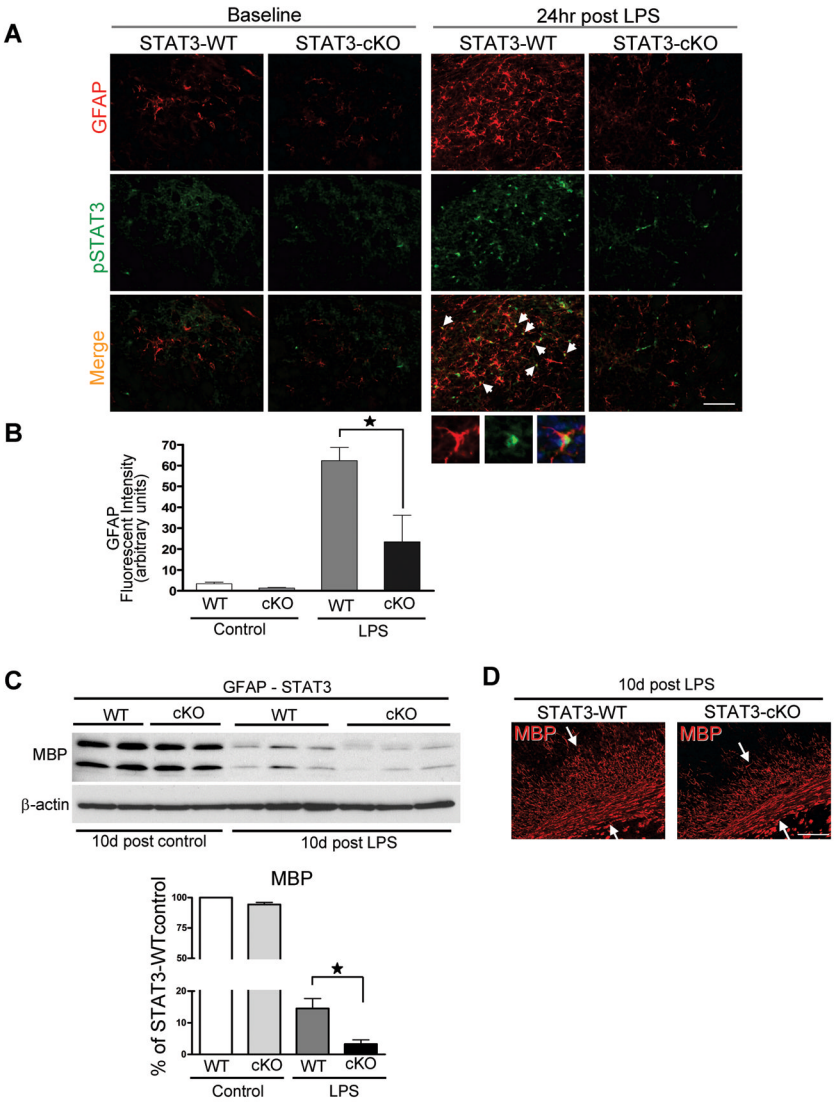

Figure 3. Conditional deletion of STAT3 gene in astrocytes reduces hypertrophic reactive astrogliosis in LPS-treated STAT3 cKO vs. WT mice, and exacerbates myelin loss after LPS injection

(A) At 24 hrs post LPS injection, WT mice show upregulation of GFAP and nuclear localization of pSTAT3, whereas in STAT3 cKO mice, GFAP upregulation is minimal and pSTAT3 appears only in scattered GFAP-negative cells. Scale bar = 100 um. Higher magnification shows nuclear localization of pSTAT3 in an astrocyte of an LPS-treated STAT3 WT mouse. **(B)** GFAP fluorescent intensity in the white matter (corpus callosum and striatum) at 24 hr after LPS injection revealed limited upregulation of GFAP in STAT3 cKO mice compared to WT littermates. N=3 in each group. **(C)** A representative Western blot for MBP in extracts of forebrains of STAT3 cKO and WT littermates collected 10 days after LPS injection shows enhanced loss of MBP protein in STAT3 cKO mice. Percent reduction in MBP (shown below) was calculated by Western blot densitometry analysis using ImageJ, taking WT control as 100%. P-values represent * <0.05. N=5–8 in each group. **(D)** Reduced MBP immunoreactivity in the corpus callosum and in cortical radiation from corpus callosum was observed in STAT3 cKO 10 days after LPS injection. Scale bar = 100 um.

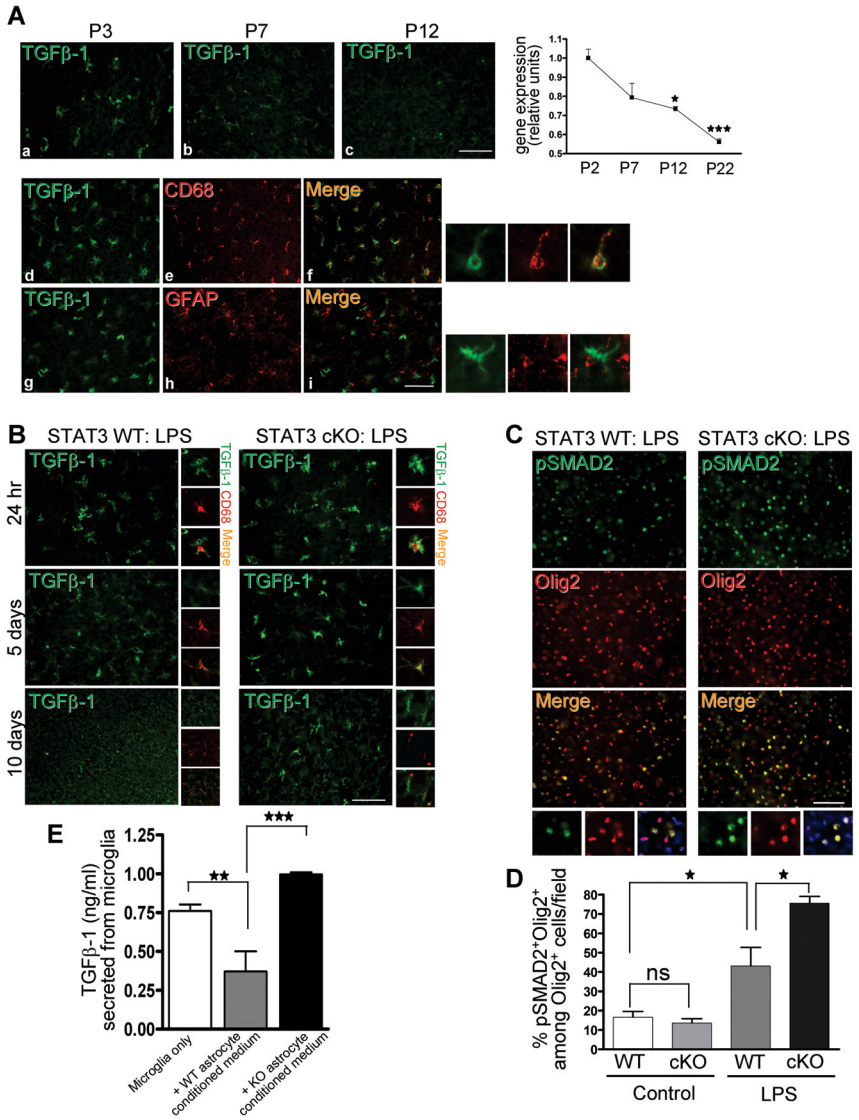

Figure 4. Expression of TGFβ-1 is developmentally regulated and perturbed after LPS injection depending on the STAT3 genotype in astrocytes

(A) a–c: In non-injected mice, declining levels of TGFβ-1 immunoreactivity were observed in the cortex and striatum between P2, P7 and P12. Scale bar = 100 um. d–i: Nearly all TGFβ-1 expressing cells were found to be $CD68^+$ microglia and no colocalization was found in $GFAP^+$ cells examined at any time point (P2, P7, and P12, P2 shown). Scale bar = 100 um. Right panel: Age-dependent decrease in TGFβ-1 was also confirmed at gene expression level (N=3–4 at each time point). P-values represent * <0.05, ***<0.001. **(B)** After LPS injection, the decline in TGFβ-1 immunoreactivity was delayed in WT mice. In STAT3 cKO mice, the reduction was even further delayed, so that levels at 10 days remained easily detectable by immunohistochemistry. Scale bar = 100 um. **(C)** Expression of phosphorylated SMAD2 in OL lineage cells 5 d after LPS injection in cortices of WT vs. STAT3 cKO mice. N=3–4 in each group. Scale bar = 100 um. **(D)** Analysis of pSMAD2 labeling indexes revealed similar percentages of $Olig2^+$ cells that were $pSMAD^+$ in non-injected WT and cKO mice, an increase after LPS injection, and a more pronounced increase in cKO mice. P-values represent * <0.05. **(E)** Secretion of TGFβ-1 from purified

C57/Bl6 WT microglia was dependent on STAT3 signaling of astrocytes. Conditioned medium from STAT3-KO astrocytes resulted in increased secretion of TGFβ-1 from microglia. In order to exclude the possibility that TGFβ-1 secreted from astrocytes confounded the results, TGFβ-1 in astrocyte conditioned media before addition to microglia was subtracted from total TGFβ-1 detected after incubation with microglia. N=4 in STAT3-WT and KO astrocyte conditioned media, experiments were repeated four time yielding similar results. P-values represent ** <0.01, ***<0.001.

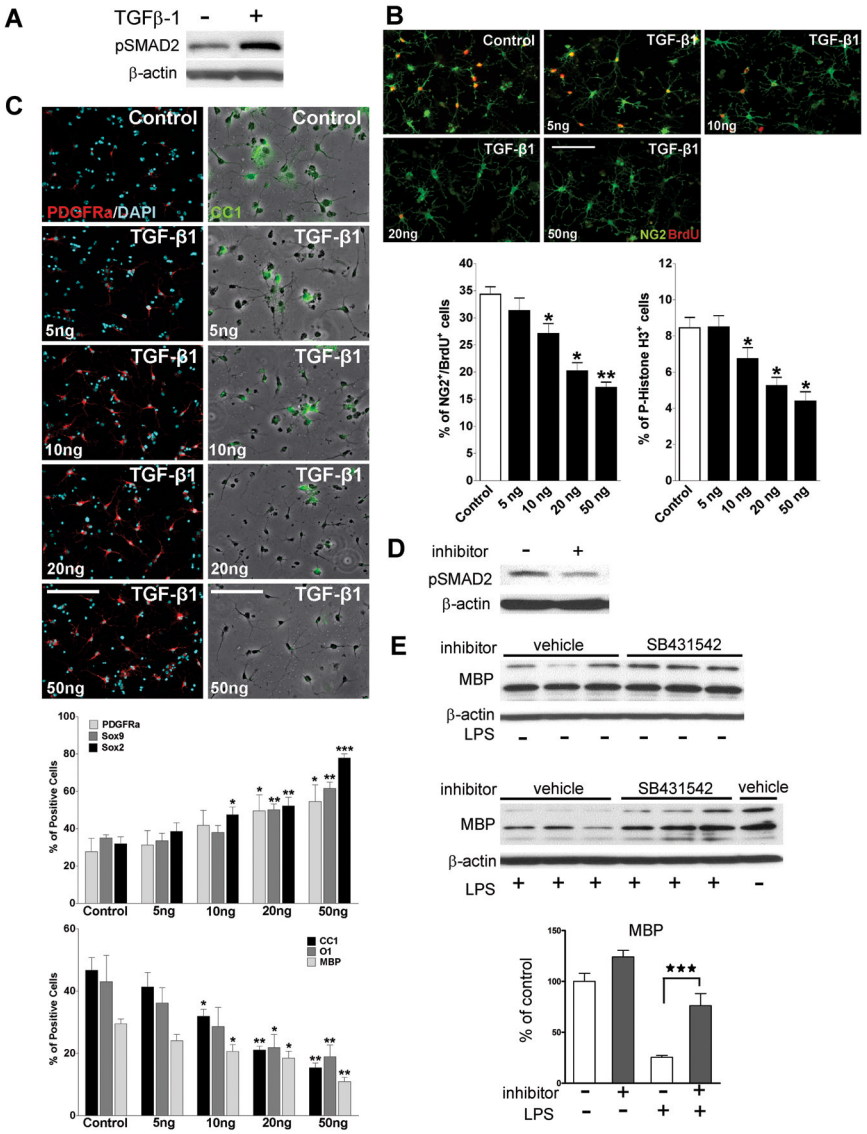

Figure 5. TGFβ-1 directly inhibits maturation of OL precursors in culture, and pharmacological antagonist of TGFβ-1 partially rescues delayed myelin development *in vivo*

(A) Purified OL progenitors responded to exogenous TGFβ-1 in culture. Western blot shows an upregulation of pSMAD2 expression 2 hours after application of 50 ng/ml TGFβ-1 in culture media. (B) Exogenous application of TGFβ-1 inhibits OL proliferation. OL progenitors were kept in culture media containing mitogens PDGF-A and bFGF for 24h and then co-treated with different concentrations of TGFβ-1 for 48h. Bromo-deoxyuridine (BrdU) 10 μM was included in the medium the last 24 hr. A dose-dependent decrease in the proliferation of NG2+ OL progenitor was observed. Values are mean ± SEM from four independent experiments. Scale bar = 40 μm. P-values represent * <0.05, ** <0.01. **(C)** Medium lacking mitogens but containing different concentrations of TGFβ-1 was added for 48h to test differentiation. Cells were then stained with antibodies against PDGFRα, Sox9, Sox2, CC1, O1 and MBP, and quantified as described in method. A dose-dependent decrease in the proportion of OL that express mature markers (CC1, O1, MBP) and increase in OL that express immature markers (PDGFRα, Sox9, Sox2) was observed. Values are mean ± SEM from four independent experiments. Scale bars = 80 μm. P-values represent *

<0.05, **<0.01, ***<0.001. **(D)** Efficacy of pharmacological blockade of TGFβ-1 was tested *in vivo* using a selective kinase inhibitor SB431542. A reduction of phosphorylated SMAD2 was observed in Western blot in the brain samples collected after 3 days after intraperitoneal injection of SB431542 (5 mg/kg) at P2. **(E)** SB431542 was administered at P2 in naive controls or mice injected with LPS, then mature myelin protein MBP was measured by western blot at P16 (14 days post injection). Whereas a marginal, non significant increase in MBP was observed in naive mice injected with SB431542, a partial rescue of MBP was observed in mice injected with LPS concurrently with SB431542. P-values represent ***<0.001.

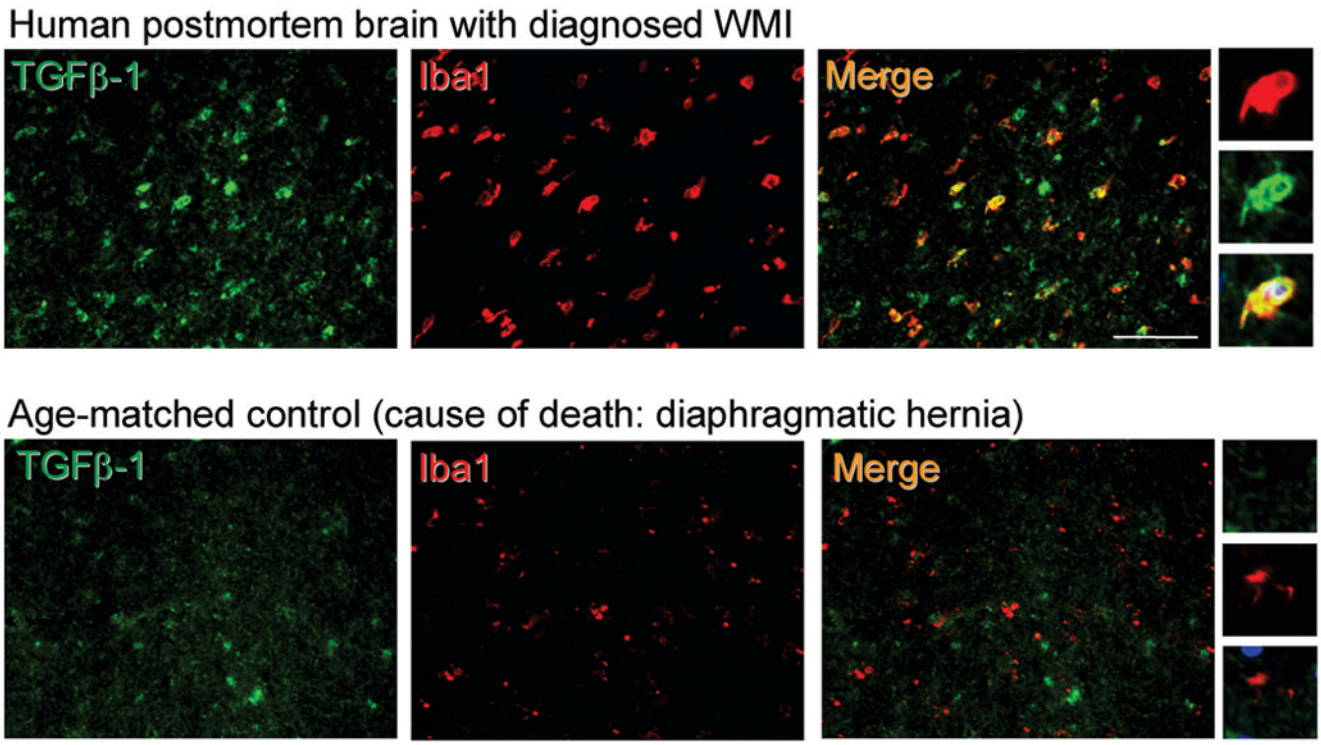

Figure 6. Human postmortem brain tissue with diagnosed hypoxia/ischemia associated WMI show upregulation of TGFβ-1 in microglia

Four cases of human WMI, (case 2 shown, also see table 1) well as three cases of age-matched control (case 6 shown) were stained for human TGFβ-1 and microglia marker Iba1. A robust microgliosis in white matter of WMI brain and colocalization of TGFβ-1 was observed. Note activated microglia with hypertrophic morphology. Scale bar = 100 um.

Table 1

Characteristics of human WMI and control samples, and activation of STAT3 pathway in astrocytes.

Case #	Diagnosis	WMI/control	Gestational age	Postnatal age	Examined area	pSTAT3 in astrocytes
1	HIE	WMI	37-4/7 wks	6 days	Subcortical WM	✓
2	HIE	WMI	35 wks	6 days	Subcortical WM	✓
3	PVL	WMI	31 wks	32 days	Periventricular WM	✓
4	PVL	WMI	38 wks	12 days	Periventricular WM	✓
5	diaphragmatic hernia	Control	36-4/7 wks	0 day	Subcortical WM	no
6	diaphragmatic hernia	Control	37-3/7 wks	2 days	Subcortical WM	no
7	Acute anoxia	Control	38 wks	2 days	Subcortical WM	no